Scientia Iranica, Vol. 15, No. 5, pp 568–574

SCIENTIA
IRANICA

Research Note

Generation of Orthoimage from High-Resolution DEM and High-Resolution Image

M. Saati[1], J. Amini[1,*], S. Sadeghian[2] and S.A. Hosseini[3]

Generating an orthoimage from high-resolution satellite images is an important undertaking for various remote sensing and photogrammetric applications. In this paper, a method is proposed that uses Artificial Neural Networks (ANN) to generate orthoimage Ikonos Geo images. For orthoimage generation, a Digital Elevation Model (DEM) with a cell size of 4 m and RMS error of 0.24 m is constructed with neural networks, based on a Quad Tree (QT) structure. In order to determine object-to-image relationships, rational function models, polynomials and neural networks with back propagation learning algorithms were used. Ground Control Points (GCPs) and check points were taken from topographic maps of 1:2000, with a contour interval of 2.5 m, to evaluate the accuracy of DEM and object-to-image transformations. The method described in this paper is tested with an Ikonos Geo image from a region of Bilesavar, Iran.

INTRODUCTION

Digital orthoimages are proving to be suitable for a variety of mapping, Geographic Information Systems (GIS) and environmental monitoring tasks. Increased demand is sparked by the availability of hardware and software suitable for use in a desktop mapping environment. The transition to softcopy photogrammetry has resulted in photogrammetric operations becoming an integral part of GIS database construction tasks. In particular, digital orthoimages are now recognized as valuable "base map" coverage that can be used to identify ground control, update existing coverage for land use/cover and transportation routes and assess changes in the landscape caused by construction or environmental phenomena [1].

In addition, orthoimages can be used as navigational tools for visualisation and as parts of multimedia information systems. Such tools are of essential value for emergency planning, crisis management and change-detection procedures in devastated areas, due to any natural disasters (floods, forest fires, earthquake devastation, volcanic eruption, etc.), as well as for all areas, especially inaccessible ones without proper maps [2]. Schiewe [3] and Meinel and Reder [4] reported first experiences with Ikonos images for topographic mapping and map updating and postulated their applicability at scales of 1:10,000 and smaller.

A number of papers in orthoimage generation from digitized aerial photos ([5,6]), air born multispectral scanner images [7] and satellite images [8] have been reported.

The orthorectification process converts images into maps by removing all orientation elements of sensor and terrain effects. In order to georeference images acquired with space-born sensors, two different approaches have been developed: Parametric and non-parametric models [9].

Tao and Hu [10] used rational functions for the relation between Ikonos Geo-images and the national coordinate system. They undertook the relationship between the scene position with 3D ground coordinates and a Rational Function (RF) of degree 3.

Rau and Chen [11] used aerial orthoimaging for geometrical building modeling. To generate a true orthoimage, they combined building models with the Digital Terrain Model (DTM) to form a Digital Surface Model (DSM).

Vassilopoulou et al. [2] used orthophoto generation with Ikonos imagery and high resolution DEM.

1. *Department of Geomatics Engineering, Faculty of Engineering, University of Tehran, P.O. Box 11365-4563, Tehran, Iran.*

2. *Research Institute of National Cartographic Center (NCC), P.O. Box 13185-1684, Tehran, Iran.*

3. *Department of Electronical Engineering, Islamic Azad University of Islamshahr, Iran.*

*. *To whom correspondence should be addressed. E-mail: jamini@ut.ac.ir*

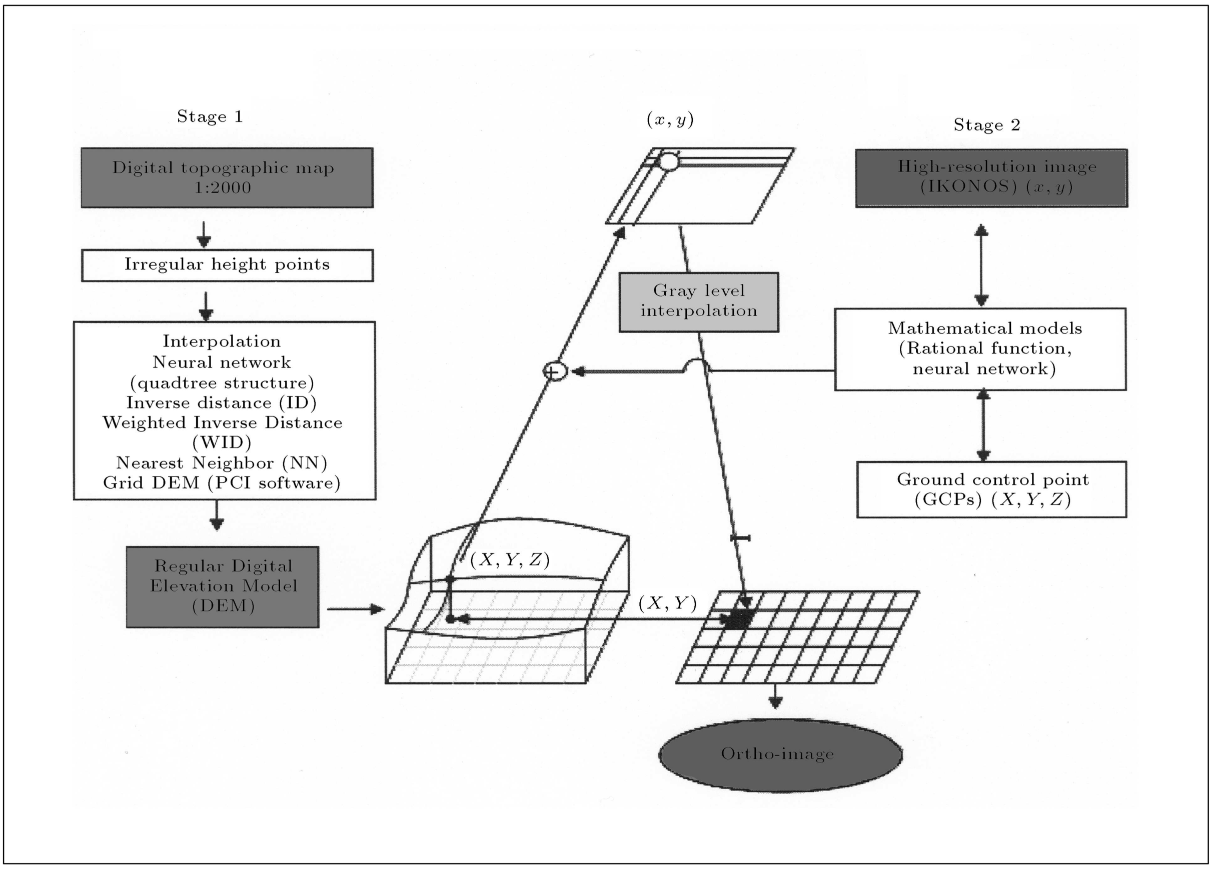

Figure 1. The algorithm for orthoimage generation.

They used a DEM with a cell size of 2 m and 38 selected GCPs measured with a Differential Global Positioning System (DGPS). Two different models: A relief-corrected affine transformation and the polynomial mapping functions of Kratky were used for an object-to-image relationship.

The correction of images derived from the NOAA/AVHRR is described by Brush [12], Crawford et al. [13] and Moreno and Melia [14]. The use of DEM to correct images for the geometric distortion produced by relief variations is considered by Blaser and Caloz [15] and Itten and Meyer [16]. Other useful references are [17-19].

The main aim of this paper is the orthorectification of a 4 m resolution Ikonos Geo-image from a region of Bilesavar, Iran. To achieve the objectives of this research, a DEM, some GCPs and an object-to-image space transformation were used. Accuracy of the object-to-image transformations (polynomials, rational functions and neural networks) was verified by GCPs and check points (CPs).

Figure 1 shows the method used to generate the orthoimage described in this paper. As indicated in this figure, the orthoimage can be generated in two parallel stages. The first stage is DEM generation, based on topographic maps of 1:2000; and the second stage is the determination of mathematical models for an object-to-image relationship based on GCPs. The results of these two stages were integrated to generate the orthoimage proposed in this paper.

The distinguishing feature of this paper is the utilization of ANN as the interpolating function model, in order to generate the DEM and produce the orthoimage. A model to determine the space relationship between the object and its related image was also proposed.

IMAGE DATA AND GCPS

The Ikonos satellite (launched in September 1999) is the world's first commercial satellite offering high-resolution imagery. Ikonos data include 1-m panchromatic, 4 m multispectral images involving three spectral channels (R, G, B) and an NIR channel. Ikonos is quick to point at any azimuthal direction with an elevation typically larger than 45 degrees. Data are collected at 11 bits; however, in reality, a much smaller range than 2048 grey values is covered in each image. The Geo product is the least expensive image and is geometrically corrected using bicubic interpolation to a cartographic projection and a reference ellipsoid, without the use of GCPs or DEM for the geocoding. More details on Ikonos can be found at www.spaceimaging.com.

In this project, a 4 m multispectral Ikonos satellite image from a region of Bilesavar, located in the northwest of Iran was used as a field test.

Figure 2a shows the image and Figure 2b illustrates the distribution of GCPs and CPs. Any CPs and GCPs with their coordinates both in the image and maps were manually derived from image and digital topographic maps with a scale of 1:2000 that was produced by the National Cartographic Centre (NCC) of Iran. It provides approximately 50 cm planimetric accuracy and 2 m vertical accuracy. In comparison with the ground resolution of the Ikonos image, this digital map provides sufficient control data. Table 1 presents the main characteristics of the acquired image.

OBJECT-TO-IMAGE SPACE TRANSFORMATION

To generate the orthoimage, a relationship between object and pixel space needed to be established. This relationship is usually determined by the exterior orientation with the use of extended co-linearity equations and GCPs. Since Space Imaging (SI) does not release information about the sensor model and no Rational Polynomial Coefficients (RPC) were available at that time, alternative sensor models had to be used.

The polynomial, Rational Function (RF) and ANN were used to determine the relationship between the image space and the GCPs. Since polynomial models did not produce the desired accuracy, the results were not included in tabulated data. In the RF models, as indicated in Equation 1, first the unknown coefficients were determined with distributions 40, 20, 15, 12 and 10 control points for each model, with different coefficients $3, 4, 5, \cdots, 13$ (coefficient 3 means that a RF model was used with terms: $a_0, a_1, a_2, b_0, b_1, b_2, \cdots, d_2$, and similar terms were used for other coefficients).

$$x = \frac{a_0 + a_1X + a_2Y + a_3Z + a_4XY + \cdots}{c_0 + c_1X + c_2Y + c_3Z + c_4XY + \cdots},$$

$$y = \frac{b_0 + b_1X + b_2Y + b_3Z + b_4XY + \cdots}{d_0 + d_1X + d_2Y + d_3Z + d_4XY + \cdots}. \qquad (1)$$

Then, with the determined coefficients, the image (pixel) coordinates of the checkpoints were calculated for 40-70 checkpoints as shown in Table 2. Based on the calculated and map coordinates for checkpoints, the RMS errors were calculated for each model. The results of these calculations are presented in Table 2.

As can be seen in Table 2, coefficient 4 produces the least RMS errors for the different distribution of control points and checkpoints. Therefore, the model with coefficient 4 is the most suitable for object-to-image space transformations.

The third model is the ANN. The ANN includes three layers: Input, output and hidden. The input layer includes three neurons (a, b, c) that correspond to the object coordinates (X, Y, Z), respectively. The output layer includes two neurons (e, f) that correspond to the image coordinates (x, y), respectively.

In the hidden layer, neurons with different distributions $(1, 2 \cdots 20)$ were used to obtain the number of neurons that produce the least RMS errors (5 neurons), as indicated in Table 3. The least RMS error, in turn, gives the best network. The results are depicted in Figure 3.

Therefore, in this paper, a network with 3 input neurons, 5 hidden neurons and 2 output neurons (or a network 3-5-2) was selected as the optimum network.

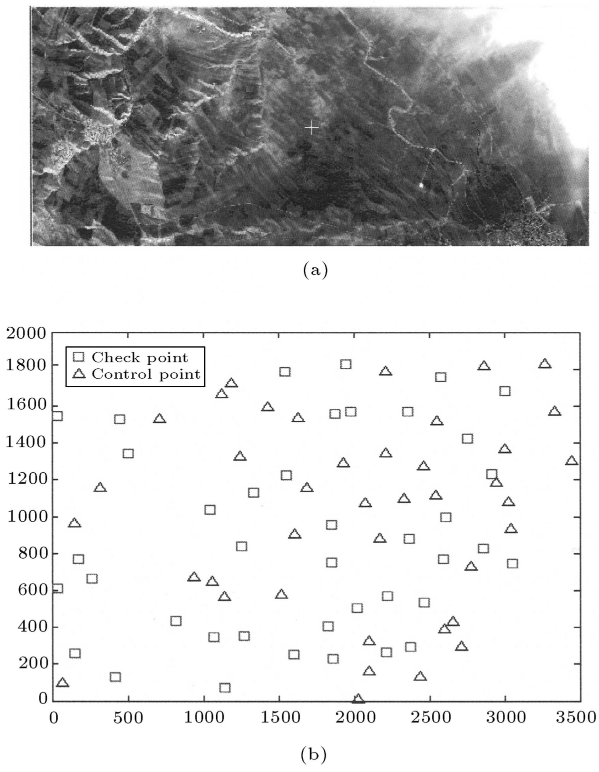

Figure 2. (a) The original image; (b) Control points and check points distribution.

Table 1. Technical specification of the Ikonos image.

Image Type	Datum	Map Projection	Size (km)	(ϕ, λ)	File Format
4-m multispectral	WGS 84	UTM	7.6*11	48°20′, 39°25′	Geo TIFF

Table 2. RMSE (pixel) result from rational polynomial models.

Number of GCPs	Number of CPs	Rational Polynomials Coefficients										
		3	4	5	6	7	8	9	10	11	12	13
40	40	2.15	1.55	1.71	1.74	1.82	1.83	1.81	2.00	1.97	2.23	2.14
20	60	2.55	1.93	1.86	1.85	1.94	1.98	2.28	4.18			
15	65	2.57	1.99	2.22	2.64	4.53	5.70	—				
13	67	2.51	2.03	2.69	4.96	7.40	—					
10	70	2.71	2.21	2.29 —								

Table 3. RMSE in the trained networks.

Number of Neurons	RMSE for GCP (pixel)	RMSE for CP (pixel)
1	782.3235	794.7373
2	1.7977	2.9516
3	1.8411	3.9828
4	2.0139	4.7708
5	1.1207	2.5918
6	1.7184	7.698
7	2.2448	4.19
8	1.8666	10.0848
9	1.5611	40.4486
10	1.0431	3.502
11	1.6287	12.5311
12	1.0127	123.0175
13	1.3869	46.5271
14	2.0163	66.2547
15	1.3169	213.6895
16	1.4699	95.4941
17	1.9634	47.7555
18	1.5263	65.5672
19	1.0483	195.5224
20	0.574	220.2096

Table 3 shows RMS errors for 40 control and 40 checkpoints for all cases.

The training parameters that were used for each network in Table 3 are as follows:

Number of epochs:	epochs=90,
Goal of performance function:	goal=1e-006,
Initial learning rate:	lr=0.0010,
Increased learning rate:	lr_inc=1.0500,
Decreased learning rate:	lr_dec=0.7000,
Magnitude of gradient:	min_grad=1.0000e -008
Training time:	time=Inf.

A comparison of results presented in Tables 2 and

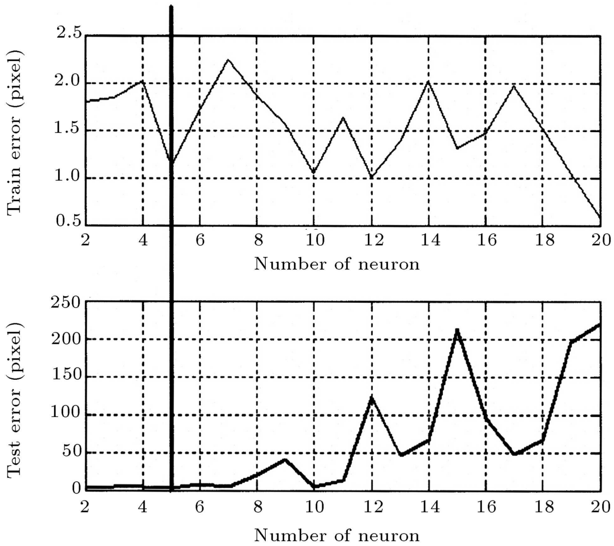

Figure 3. Number of neurons with different distribution.

3 reveals that a RF model with 4 coefficients produces less RMS errors than ANN models 3-5-2.

GENERATION OF DEM FROM TOPOGRAPHIC MAPS 1:2000

The use of a DEM is important for any environmental study of a region. It represents an important component (3D terrain representation) of maps and GIS databases and serves as a base for thematic applications (geologic, tectonic), ortho-photo generation and for the production of a great variety of maps, including 3D maps, slope-aspect maps and others.

The applied methodology for obtaining a DEM depends on numerous parameters. These parameters include type of data (contours, points, drainage network, etc.) and the quality and density of the data that is related to the morphology of the study area. The obtained DEM depends on the parameters of the applied algorithm, the dimension of the DEM (i.e. the pixel size of the regular grid to be interpolated) and the scale of the map in which the DEM is represented etc. [2,20,21].

For this study, the input data required to produce the DEM were taken from topographic maps of 1:2000 with contour intervals of 2.5 m and the number of elevation points. For the given data, interpolation methods were utilized to generate regular DEMs with a cell size of 2 m. Interpolation methods consisted of ANN, Simple Inverse Distance (SID), Weighted Inverse Distance (WID), Nearest Neighbour (NN) and Grid DEM in PCI Geomatica software.

A method based on a Multi Layer Perceptron Neural Network (MLPNN) and a QT structure was proposed as an interpolating method to generate DEM.

The input data collected for this study is approximated to be about 1.5 million irregular points. To make the number of input data more manageable for DEM generation, a quad tree structure was used to cluster the irregular points to patches. This structure resulted in 1800 separate clusters with a maximum of 2000 points in each patch. ANN was applied to each cluster to form the patches. MLPNN consists of three layers, namely, an input layer with two neurons, a hidden layer with five neurons and an output layer with one neuron. The two neurons in the input layer correspond to the coordinates of the x and y points. The one neuron in the output layer corresponds to the z of the points. Figure 4 shows the quad tree structure that was applied to the irregular points to form the clusters and patches.

The patches formed above by MLPNN were used to generate DEM.

To make a quantitative evaluation of the generated DEMs with different interpolation methods, 20 points were selected from a topographic map. The Root Mean Square (RMS) error for these points in each interpolating method was calculated and is presented in Table 4. The accuracy of the MLPNN method is 0.24 m and the PCI Geomatica method is 0.20 m. The results reveal that the ANN accuracy is fairly close to the method in PCI software. Adding the training data and changing the network parameters, however, can improve the accuracy of the method.

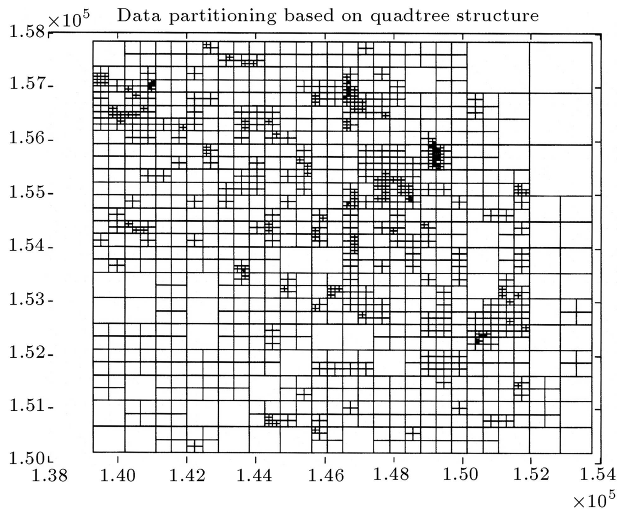

Figure 4. Quad tree structure applied on the irregular points to form the clusters.

ORTHOIMAGE GENERATION

Figure 1 shows the flow diagram for generating the orthoimage proposed in this research. As indicated in the diagram, stage 1 provides the methodologies for generating DEM, while stage 2 leads to the development of mathematical models. When the results in stages 1 and 2 are integrated, a high-resolution orthoimage can be generated.

To generate the orthoimage, first each node of DEM (X, Y, Z) that was generated with the proposed method, by using the rational function with coefficient 4, is transformed into pixel space (x, y). Then, the bilinear grey value interpolation is performed to obtain a grey value for that node in the space image. This grey value is assigned to the node of the regular grid in coordinates (X, Y). This process is sequentially repeated for all the nodes of DEM (Figure 5a), to produce the orthoimage that is shown in Figure 5b.

In order to evaluate the generated orthoimage, 93 GCPs with ground coordinates X, and Y, were selected from the map. The Image coordinates for the GC points were also manually extracted from the

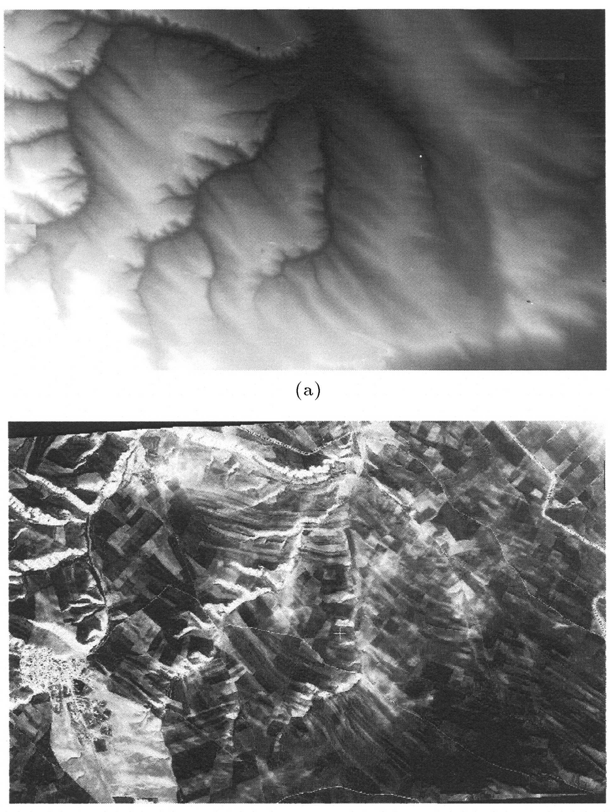

Figure 5. (a) DEM generation with quad tree structure. (b) Orthoimage.

Table 4. DEM interpolated accuracy and RMS errors.

Number of Points	RMS Error (MLPNN)	RMS Error (PCI)	RMS Error (NN)	RMS Error (SID)	RMS Error (WID)
20	0.24	0.20	0.38	0.67	0.41

orthoimage. Based on two types of coordinate (map coordinates and orthoimage coordinates), the RMS error depicted in Table 5 was calculated.

Finally, based on Equation 2, the scale of map that can be produced from the generated orthoimage is calculated in Table 6.

$\sigma_{\mathrm{Pl}}(\mathrm{m}) = \text{Scale number} * 0.3(\mathrm{mm}),$

where:

$$\text{Scale of map} = 1/\text{Scale number}. \tag{2}$$

CONCLUSION

The orthoimages with high resolution and, specifically, the ortho-Ikonos images (1-m resolution) can provide useful information regarding the geology and the geodynamics of a region. It can also contribute to various Geo-environmental applications, both in the laboratory and in the field.

These corrected satellite images may be used in the following domains and serve various purposes, such as the production of various ortho-maps relating to topography, land use, tectonics, Geo-tectonics, morphotectonics, geology and geomorphology, and a base map for the location of the GPS measurements or stations in applied disciplines of geosciences (geophysics, seismology, geothermic, geochemistry, hydrogeology), both in the field and the laboratory.

Subsequently, these corrected images can be used as navigational tools for emergency planning, in crisis management and evaluation procedures in devastated areas, due to natural disasters such as floods, forest fires, earthquake devastation and volcanic eruption, as well as being a useful tool for all non-accessible areas without proper maps.

In this paper, an IKONOS Geo image was used for orthoimage generation. For orthoimage generation, a DEM with sufficient accuracy and a suitable model for an image-to-object relationship is needed. This paper investigated the capability of ANN for DEM generation and an image-to-object relationship. Using ANN for DEM generation had better results than the image-to-object relationship. This is due to the training data having an important role in ANN. In DEM generation, training samples can be simply taken from a lot of irregular points. For an image-to-object relationship, because there are few GCPs, one is limited to these points, which is not adequate for training the ANN. To make the amount of input data more manageable for DEM generation, a QT structure was used to cluster the irregular points to patches. The ANN was applied to each cluster to determine the regular points in DEM. This method was compared with interpolation methods consisting of SID, WID, NN and Grid in PCI software. The ANN had better results than other methods. Only the Grid method in PCI software give the results nearly close to the ANN method.

For an image-to-object relationship, rational function, polynomials and neural networks were used. The GCPs were taken from topographic maps in a scale of 1:2000. These points can also be provided by GPS. The rational function with four coefficients had better results than the other models. Finally, it was shown that, if the method described in this paper were used, it would be possible to produce an orthoimage or a map with a scale of 1:12000 with a planimetric accuracy of 3.41 m.

Table 5. The accuracy of the orthoimage.

Number of Points	RMS Error(pixel)
93	3.41

Table 6. A map that can be produced with the generated orthoimage.

Method	σ_{Pl} (m)	Scale of Map
RF with ANN	3.41	1:12000

REFERENCES

1. Welch, R. and Jordan, T.R. "Digital orthophoto production in a desktop environment", *GIM Magazine*, **10**(7), pp 26-27 (July, 1996).
2. Vassilopoulou, S., Hurni, D., Dietrich, V., Baltsavias, E. Pateraki, M. Lagios, E. Parcharidis, I. "Orthophoto generation using IKONOS imagery and high resolution DEM", *ISPRS Journal of Photogrammertiy & Remote Sensing*, **57**, pp 24-38 (2002).
3. Schiewe, J. "Potenzial und probleme neuer hochauflösender weltraumsensoren für kartographische anwendungen", *Kartographische Nachrichten*, **51**, pp 273-278 (2001).
4. Meinel, G. and Reder, J. "IKONOS satellitenbilddaten-ein erster erfahrungsbericht", *Kartographische Nachrichten*, **51**, pp 40-46 (2001).
5. Wiesel, J.W. "Digital image processing for orthophoto generation", *Photogrammetria*, **40**(2), pp 69-76 (1985).

6. Hohle, J. "Experiences with the production of digital orthophoto", *PE & RS*, **62**(10), pp 1189-1194 (1996).

7. Chen, N.Y., Wang, H.T. and Lin, M.M. "Orthographic correction of airborne scanner imagery for mountainous areas", *Proc. of the 3rd International Airborne Remote Sensing Conference and Exhibition*, Copenhagen, Denmark, 7-10 July, **II**, pp 293-299 (1997).

8. Chen, J.C. and Lee, L.H. "Rigorous generation of digital orthophotos from SPOT images", *PE & RS*, **59**(3), pp 655-661 (1993).

9. Gianinetto, M., Giussani, A., Lechi, M. and Scaioni, D.M. "Fast mapping from high resolution satellite images: A sustainable approach to provide maps for developing countries", *International Archive of Photogrammetry, Remote Sensing and Spatial Information Sciences*, **XXXV**, part B, ISPRS 12-23 July, Istanbul, Turkey (2004)

10. Tao, C.V. and Hu, Y. "3D reconstruction methods based on the rational function model", *PE & RS*, **68**(7), pp 705-714 (2002).

11. Rau, J. and Chen, L. "Geometrical building modeling and its application to the ortho-rectification for aerial images", *Journal of Photogrammetry and Remote Sensing*, **9**(1), pp 53-76 (2004).

12. Brush, R.J.H. "A method for real-time navigation of AVHRR imagery", *IEEE Transactions on Geoscience and Remote Sensing*, **23**, pp 876-887 (1985).

13. Crawford, P.S., Brooks, A.R. and Brush, R.J.H. "Fast navigation of AVHRR images using complex orbital models", *International Journal of Remote Sensing*, **17**, pp 197-212 (1996).

14. Moreno, J.E. and Melia, J. "A method for accurate geometric correction of NOAA AVHRR HRPT data", *IEEE Transactions and Geoscience and Remote Sensing*, **31**, pp 204-226 (1993).

15. Blaser, T.J. and Caloz, R. "Digital orthoimage registration from a SPOT panchromatic image using a digital elevation model", *IEEE Trans. Geosci. on Remote Sensing*, **29**, pp 2431-2434 (1991).

16. Itten, K.I. and Mayer, P. "Geometric and radiometric correction on TM data of mountainous forested areas", *IEEE Trans. Geosci. Remote Sensing*, **31**, pp 764-770 (1993).

17. Fogel, D.N. and Tinny, L.R. "Image registration using multiquadric functions, the finite element method, bivariate mapping polynomials and tin plate spline", *Technical Report 96-1*, University of New York, and University of Maine (1996).

18. Kardoulas, N.G., Bird, A.C. and Lawan, A.I. "Geometric correction of SPOT and Landsat imagery", *PE & RS*, **62**, pp 1173-1177 (1996).

19. Cook, A.E. and Pinder, J.E. "Relative accuracy of rectifications of coordinates determined from maps and global positioning system", *PE & RS*, **62**, pp 73-77 (1996).

20. Vassilopoulou, S. "Geodynamics of the Argolis peninsula with GIS development and the use of remote sensing data", PhD Thesis, University of Athens, Faculty of Geology, p 194 (1999).

21. Vassilopoulou, S. and Hurni, L. "The use of digital elevation models in emergency and socio-economic planning: A case study at Kos-Yali-Nisyros-Tilos islands, Greece", *Proc. 20th International Cartographic Conference*, Beijing, China, Chinese Society of Geodesy, Photogrammetry and Cartography, pp 3424-3431 (2001).